Atmosphere-Ocean

Publication details, including instructions for authors and subscription information:
http://www.tandfonline.com/loi/tato20

Interannual variability of sea-ice cover in Hudson bay, Baffin bay and the Labrador sea

Jia Wang [a c], Lawrence A. Mysak [a] & R. Grant Ingram [b]

[a] Centre for Climate and Global Change Research, McGill University, 805 Sherbrooke Street West, Montréal, Quebec, H3A 2K6

[b] Department of Atmospheric and Oceanic Sciences, McGill University, 805 Sherbrooke Street West, Montréal, Quebec, H3A 2K6

[c] Physical and Chemical Sciences, DFO, Bedford Institute of Oceanography, P.O. Box 1006, Dartmouth, N.S., B2Y 4A2

Version of record first published: 19 Nov 2010.

To cite this article: Jia Wang, Lawrence A. Mysak & R. Grant Ingram (1994): Interannual variability of sea-ice cover in Hudson bay, Baffin bay and the Labrador sea, Atmosphere-Ocean, 32:2, 421-447

To link to this article: http://dx.doi.org/10.1080/07055900.1994.9649505

Interannual Variability of Sea-Ice Cover in Hudson Bay, Baffin Bay and the Labrador Sea

Jia Wang*, Lawrence A. Mysak and R. Grant Ingram
Centre for Climate and Global Change Research

and

Department of Atmospheric and Oceanic Sciences
McGill University, 805 Sherbrooke Street West
Montréal, Quebec H3A 2K6

[Original manuscript received 4 January 1993; in revised form 29 July 1993]

ABSTRACT *The spatial and temporal relationships between subarctic Canadian sea-ice cover and atmospheric forcing are investigated by analysing sea-ice concentration, sea-level pressure and surface air temperature data from 1953 to 1988. The sea-ice anomalies in Hudson Bay, Baffin Bay and the Labrador Sea are found to be related to the North Atlantic Oscillation (NAO) and the Southern Oscillation (SO). Through a spatial Student's t-test and a Monte Carlo simulation, it is found that sea-ice cover in both Hudson Bay and the Baffin Bay–Labrador Sea region responds to a Low/Wet episode of the SO (defined as the period when the SO index becomes negative) mainly in summer. In this case, the sea-ice cover has a large positive anomaly that starts in summer and continues through to autumn. The ice anomaly is attributed to the negative anomalies in the regional surface air temperature record during the summer and autumn when the Low/Wet episode is developing. During strong winter westerly wind events of the NAO, the Baffin Bay–Labrador Sea ice cover in winter and spring has a positive anomaly due to the associated negative anomaly in surface air temperature. During the years in which strong westerly NAO and Low/Wet SO events occur simultaneously (as in 1972/73 and 1982/83), the sea ice is found to have large positive anomalies in the study region; in particular, such anomalies occurred for a major portion of one of the two years. A spectral analysis shows that sea-ice fluctuations in the Baffin Bay–Labrador Sea region respond to the SO and surface air temperature at about 1.7-, 5- and 10-year periods. In addition, a noticeable sea-ice change was found (i.e. more polynyas occurred) around the time of the so-called "climate jump" during the early 1960s. Data on ice thickness and on ice-melt dates from Hudson Bay are also used to verify some of the above findings.*

RÉSUMÉ *On étudie la relation temporelle et spatiale entre la couverture de glace de mer du subarctique canadien et le forçage atmosphérique en analysant les données sur la concen-*

*Present affiliation: Physical and Chemical Sciences, DFO, Bedford Institute of Oceanography, P.O. Box 1006, Dartmouth, N.S. B2Y 4A2.

ATMOSPHERE-OCEAN 32 (2) 1994, 421–447 0705-5900/94/0000-0421$01.25/0

tration glacielle, la pression au niveau de la mer et la température de l'air en surface pour la période 1953–1988. On constate que les anomalies glacielles dans la baie d'Hudson, la baie de Baffin et la mer du Labrador sont associées aux oscillations nord-atlantique (NAO) et australe (SO). L'utilisation d'un test spatial de Student et d'une méthode de Monte Carlo montre que la couverture glacielle tant dans la baie d'Hudson que dans la région de la baie de Baffin et de la mer du Labrador réagi à un épisode «bas/humide» de la SO (lorsque l'indice SO devient négatif) surtout durant l'été. Dans ce cas, la glace de mer a une forte anomalie positive qui débute en été et se continue jusqu'à l'automne. L'anomalie glacielle dépend du fait que l'anomalie de la température de l'air en surface au niveau régional est négative en été et en automne lorsque l'épisode bas/humide se développe. Les forts vents d'ouest hivernaux de la NAO entraînent une anomalie positive de la couverture glacielle de la baie de Baffin et de la mer du Labrador, en hiver et au printemps, en raison de l'anomalie négative associée de la température de l'air en surface. Au cours des années, où simultanément, de forts vents d'ouest de la NAO et d'épisodes bas/humides de la SO se présentent (comme en 1972/73 et 1982/83), la glace de mer a de fortes anomalies positives dans la région étudiée; en particulier, de telles anomalies se sont présentées pour une grande partie d'une des deux années. Une analyse spectrale montre que les fluctuations glacielles dans la région de la baie de Baffin et de la mer du Labrador réagissent à la SO et à la température de l'air en surface à environ tous les 1,7, 5 et 10 ans. De plus, on a constaté un important changement du glaciel (c.-à-d. plus de polynies) aux environs de la période dite «saut climatique» au début des années 60. L'épaisseur de la glace de mer et la date de la fonte dans la baie d'Hudson sont aussi utilisées pour vérifier certains des résultats ci-dessus.

1 Introduction

Hudson Bay is Canada's largest inland sea, which is fully ice-covered in winter and ice-free in August and September. It has two openings, Roes Welcome Sound in the north and one southeast of Southampton Island, that allow the exchange of waters with Foxe Basin and Hudson Strait, respectively (Fig. 1). If Hudson Bay is combined with the adjacent regions of Foxe Basin and Hudson Strait, the resultant area can be considered an essentially closed system that is isolated from the effects of open-ocean circulation; therefore, the changes of sea-ice cover in Hudson Bay are expected to be mainly due to atmospheric forcing. In this sense Hudson Bay differs from adjacent ocean areas such as Baffin Bay and the Labrador and Greenland seas, where both the ocean circulation and atmospheric forcing play an important role in determining the extent of ice cover (e.g. Hibler and Bryan, 1987; Mysak et al., 1990; Mysak and Power, 1992).

A relationship between sea-ice conditions in the Baffin Bay–Labrador Sea region and the large-scale atmospheric circulation in the North Atlantic region was first noted by Rogers and van Loon (1979). They found that when the Icelandic Low in January was deep and intensified, severe ice conditions occurred in Davis Strait the following spring and summer. The possible influence of Pacific atmospheric circulation anomalies on Hudson Bay–Labrador Sea ice cover could be inferred from another study published by the same authors. Van Loon and Madden (1981) showed that certain Northern Hemisphere sea-level pressure (SLP) and air temperature interannual variations were associated with the Southern Oscillation (SO) in

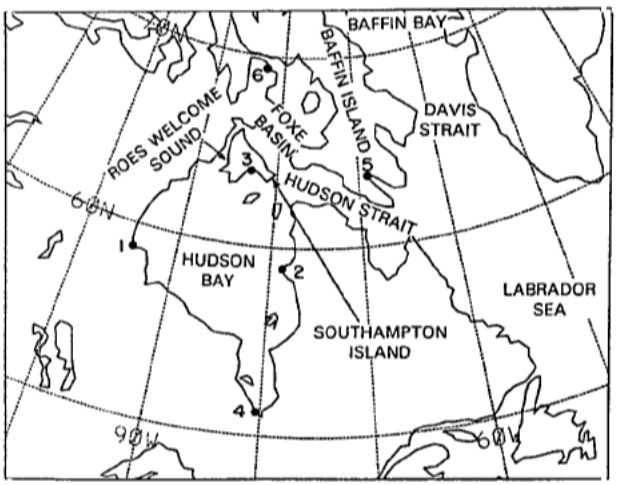

Fig. 1 The geometry of the Hudson Bay and Baffin Bay–Labrador Sea region. The numbered dots are the ice thickness stations whose data are used in Fig. 16: 1 – Churchill, 2 – Inukjuac, 3 – Coral Harbour, 4 – Moosonee, 5 – Iqaluit and 6 – Hall Beach.

the tropical Pacific. Some of these variations could be ascribed to the Pacific North American teleconnection pattern in the mid-troposphere (Bjerknes, 1969; Horel and Wallace, 1981; Mysak, 1986). This pattern of highs and lows was particularly well developed in winter 1983, following the very strong 1982/83 ENSO event. Mysak and Manak (1989) proposed that the anomalous northerly winds in eastern Canada associated with this circulation pattern, as well as a deepened Icelandic Low, were major factors contributing to the severe winter 1983 ice conditions in the Labrador Sea. A study of atmosphere-ice interactions in the Labrador Sea (as well as in parts of the Arctic) has also been recently carried out by Agnew (1993).

The existence of decadal-scale fluctuations in ice cover in the Labrador Sea was first noted by Mysak and Manak (1989; see their Fig. 18). They suggested that these fluctuations could be due to decadal-scale sea surface temperature anomalies in the northwest North Atlantic, or to the 7–8 year periodicity in the North Atlantic Oscillation (NAO). According to Rogers (1984; see his Fig. 1), the winter index of the NAO (defined as the normalized winter SLP difference between Ponta Delgadas, Azores, and Akureyri, Iceland) has exhibited this periodicity since 1960. It is interesting to note, however, that the fluctuations of sea-ice extent in Hudson Bay (Mysak and Manak, 1989; see their Fig. 17) show more of a mixed signal (i.e. both interannual and decadal variations), which suggests that they may be driven by both the SO and the NAO. However, one difference between the NAO and the SO is that the former behaves as a standing oscillation over the North Atlantic Ocean, whereas the SO is associated with global propagating SLP anomalies, monsoons and mid-latitude teleconnection patterns (Barnett, 1985). In addition, the SO appears to have two distinct periods of motion: 2 years and 3–5 years (Barnett, 1991).

In this study, we shall build on the above work and examine in more detail the

response of the sea-ice cover in Hudson Bay and the Baffin Bay–Labrador Sea region to two major atmospheric circulation patterns: the Southern Oscillation and the North Atlantic Oscillation. In particular, both the spatial and temporal scales of variability will be determined using various datasets that extend over more than three decades.

The outline of this paper is as follows. A short review of previous studies on sea-ice variations in Hudson Bay and the Baffin Bay–Labrador Sea region is given in Section 2. The data sources used in this paper are described in Section 3. In Section 4, the spatial distributions of sea-ice concentration (SIC), sea-level pressure (SLP) and surface air temperature (SAT) are examined to determine the response of sea ice to atmospheric circulation patterns. (Note: all the acronyms frequently used in this paper are defined in the Appendix.) In Section 5, the temporal variations of sea-ice cover are spectrally analysed in order to find the time-scales of variability. In Section 6, seasonal time series are used to determine the relative importance of the NAO and the SO influences on sea-ice cover using a Monte Carlo simulation; ice thickness and melting dates in Hudson Bay are also used to verify some of our findings. In Section 7, the response of sea-ice to two simultaneous strong Low/Wet SO and strong westerly wind NAO episodes are examined to further support the findings of this paper. Conclusions and a summary are given in Section 8.

2 Review of previous studies of sea-ice variability in the Arctic and Hudson Bay–Labrador Sea region

In contrast to the previously mentioned analyses of multi-decade ice-cover records, Parkinson and Cavalieri (1989) and Parkinson (1991) carried out a systematic survey of the variability of Arctic sea ice for the 15-year period 1973–87 using only passive-microwave satellite data. The study examined all Arctic regions, including Hudson Bay and the Baffin Bay–Labrador Sea region. They found that in both 1982/83 and 1986/87 ENSO events, the sea-ice cover was anomalously high in Hudson Bay and Baffin Bay/Davis Strait. This suggests that the sea-ice cover in this region may be high during Low/Wet SO episodes when the SO index is negative.

A systematic analysis of the seasonal cycle of ice conditions in Hudson Bay was presented by Danielson (1969, 1971) using field observations. In particular, relationships between sea ice and regional meteorological conditions were examined in detail. However, interannual variations were not studied. Seasonal ice thickness (Prinsenberg, 1988) and ice concentration (Markham, 1986) data have been assembled using field and satellite data. Prinsenberg found that heavy ice conditions generally occurred in northwestern Hudson Bay. Markham showed the climatological mean evolution of the ice breakup/melt in spring, ice-free condition in summer, and freeze-up in autumn. The sensitivity of ice breakup in Hudson Bay to air temperature changes was studied by Etkin (1991). The variations in sea-ice cover in southeastern Hudson Bay were determined by Larouche and Galbraith (1989) who analysed satellite images for a 13-year period (1972–85). They classified the ice

distribution into three categories: complete, half and absent fast-ice cover in the study region. Some relationships between ice cover and local wind, water circulation and air temperature were also determined.

3 The data

The data that were analysed include monthly SLP, SAT and SIC contained in the J. Walsh climate dataset from the University of Illinois. The SLP data extend from January 1899 to January 1988 and are given in grids of 5° × 5° latitude-longitude covering the Northern Hemisphere from 15°N to the north pole. The original analyses, obtained from the National Center for Atmospheric Research (NCAR), were archived twice daily (0000 and 1200 UTC) on 5° × 5° latitude-longitude grids and averaged on a monthly basis at the University of Illinois. Missing SLP data were replaced by climatological values. However, the data were fairly complete after 1953. A detailed description of the SLP data is given by Wang and Mysak (1991).

The SAT data used extend from 1954 to 1986 and are given in 5° × 5° latitude-longitude grids, covering both hemispheres. The SAT data were derived from grids of mean values created by NCAR added to the grids of surface temperature anomalies computed by Jones and Wigley at the University of East Anglia (Jones, 1988). Missing SAT data were replaced by the normals from NCAR (W.L. Chapman, pers. commun., 1990). A brief description of the SAT data is given by Walsh and Chapman (1990).

The SIC data that were available for this study extend from 1953 to 1988, and cover the Arctic Ocean and adjacent seas, with a 1° × 1° latitude-longitude grid. They were compiled from different data sources, as described by Walsh and Johnson (1979a). The missing data in particular months were replaced by the climatological values.

Two other independent sea-ice datasets, namely, ice thickness (Loucks and Smith, 1989), and weekly SIC data for Hudson Bay from the Ice Centre of the Atmospheric Environment Service (AES) of Canada, were also used to verify some of our findings. Also, ice-melt dates in Hudson Bay (Etkin, 1991) were used to study the interannual variability of ice breakup in this region.

4 Spatial variability of the SIC, SLP and SAT

a *Climatological Maps of the SIC, SLP and SAT*

Before investigating interannual variations, the seasonal SIC climatologies for the period 1953–88 were constructed (Fig. 2). Throughout this study, the computation of seasonal maps uses December-January-February as winter, March-April-May as spring, June-July-August as summer, September-October-November as autumn. The months of January–December are used for the annual mean.

Figure 2 only shows the winter and summer climatological SIC in Hudson Bay and the Baffin Bay–Labrador Sea region. There is complete ice cover in Hudson Bay in winter followed by a limited breakup (or polynya formation) in the

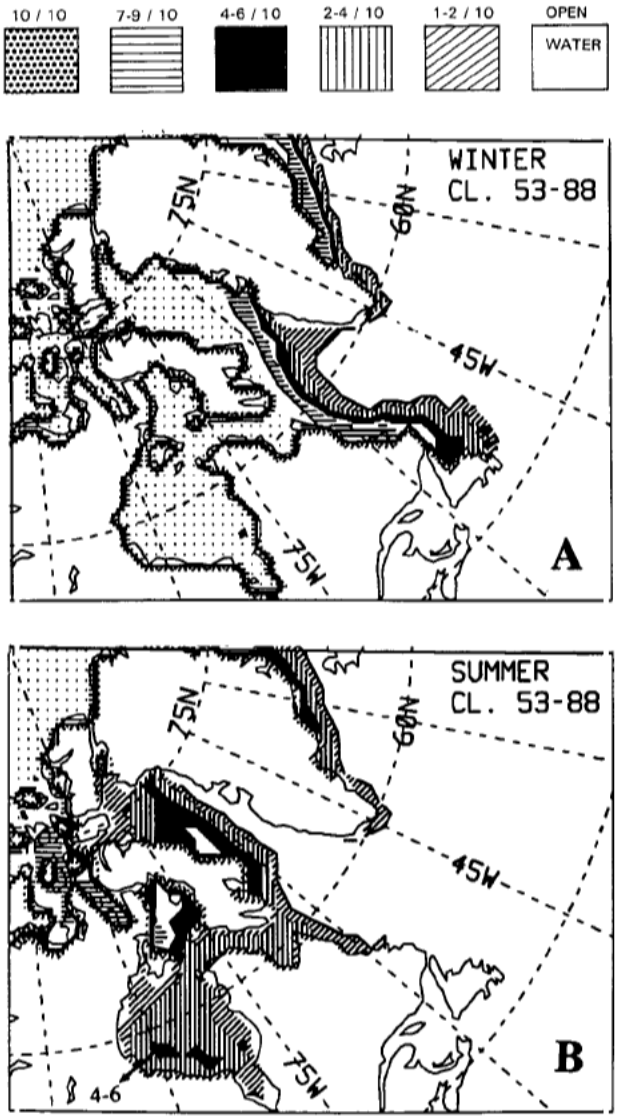

Fig. 2 The winter and summer climatological means of SIC in tenths for the period 1953–88. The same shading scheme is used throughout for all SIC maps unless otherwise specified.

northwestern and eastern portions of the bay in spring. In summer, we note the 4/10–6/10 concentration region near the southern coast of the bay. Usually, the freeze-up commences in October, advancing from north to south. In Baffin Bay, there is also a complete ice cover in winter and spring, except for some breakup in northern Baffin Bay in spring, the so-called "North Water" polynya, with values

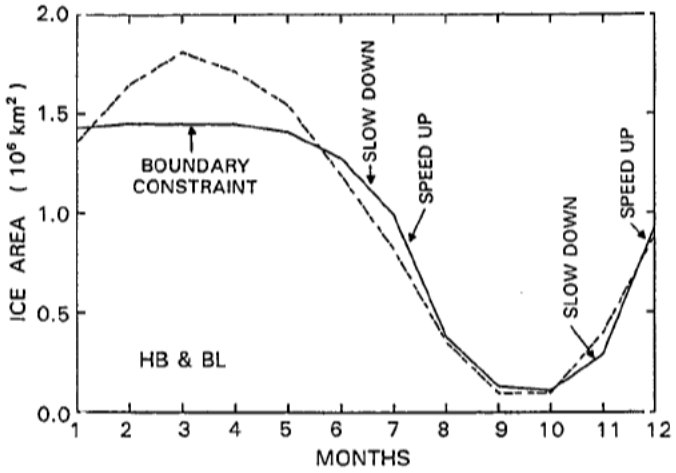

Fig. 3 The seasonal cycles for the sea-ice areas in the two regions for 1953–88. The solid (dashed) curve denotes the Hudson Bay (Baffin Bay–Labrador Sea) sea-ice area.

of 7/10–9/10 concentration. Less sea ice in winter and spring and the absence of ice in summer and autumn along the west coast of Greenland reflect the presence of the relatively warm northward-flowing West Greenland Current. Similarly, the long stretch of sea-ice extent along the Labrador-Newfoundland Shelf in winter and spring is due in part to the effect of the cold southward-flowing Labrador Current. In summer, the ice edge in the Labrador Sea retreats north to western Baffin Bay owing to the influence of the West Greenland Current. In autumn, sea ice forms from northwest to southeast.

The seasonal climatologies of SLP for 1953–87 are given by Wang and Mysak (1991). The SAT seasonal climatologies for 1953–86 (not shown) indicate a large seasonal cycle that coincides with the seasonal cycle in Hudson Bay ice cover: temperatures of −20 to −25°C in winter occur with heavy ice conditions, temperatures of −5 to −15°C in spring bring on ice breakup conditions, temperatures of about 10°C in summer help produce ice-free conditions in late summer, and temperatures of 0 to −5°C in autumn induce ice freeze-up conditions. We have found that Hudson Bay experiences a pattern of colder inland temperatures than those in the southern portion of the Baffin Bay–Labrador Sea region. In addition, the latter region shows the effects of the West Greenland Current, with warmer air temperatures all year round. Greenland SATs are below freezing year round owing to its high topography.

Figure 3 shows the climatological seasonal cycles of the monthly means of sea-ice cover in the two regions of study for 1953–88. The "boundary constraint" effect (solid ice from January to April) is seen in the Hudson Bay curve, but not in the Baffin Bay–Labrador Sea curve. The sea-ice extent in the Baffin Bay–Labrador Sea region reaches its maximum (minimum) in March (September). Breakup in

TABLE 1. Northern winters/southern summers (December-February) when the Southern Oscillation reached its extreme. High/Dry and Low/Wet refer to sea-level pressure in the tropical portions and rainfall in the equatorial region of the South Pacific Ocean. Plus/minus signs denote the strong/moderate Low/Wet episodes when SOI < 0. The data were taken from van Loon and Madden (1981), Mysak (1986) and Wakata and Sarachik (1991). The NAO episodes defined in terms of the strength of westerlies over the northern North Atlantic Ocean were taken from Rogers (1984). The asterisks, however, denote the years in which they were not defined before, but which we include as a consequence of an analysis of the recently updated SLP data.

High/Dry SOI > 0	Low/Wet SOI < 0	Weak Westerly	Strong Westerly
	1952/53–		
			1954
1954/55		1955	
55/56		56	
			57
	57/58+		
		59	
		60	
			61
61/62			
		63	
	63/64–	64	
		65	
	65/66–	66	
66/67			
		68	
	68/69–	69	
	69/70–		
70/71			
			72*
	72/73+		73
73/74			74
			75
75/76			76
	76/77–	77	
	77/78+	78	
78/79		79	
	79/80–		
			81
81/82			82*
	82/83+		83
			84*
84/85			
		86*	
	86/87–		
Sum 10	12	14	12

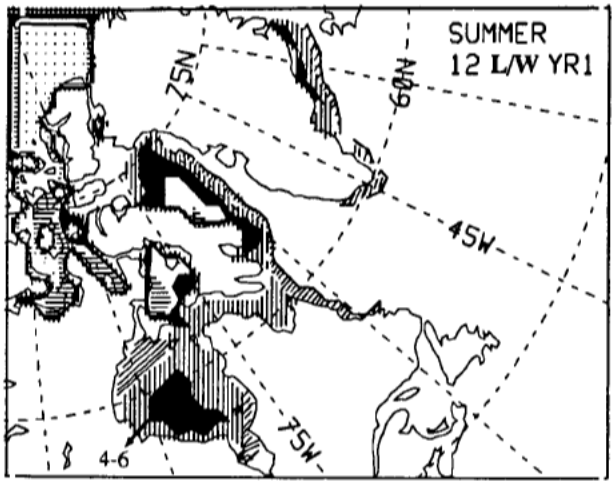

Fig. 4 The composite SIC mean of 12 Low/Wet (SOI < 0) episodes (listed in Table 1) for the first-year summer when an SO index starts to drop to negative values.

this region occurs in April. In both early spring and early autumn, sea-ice decay and formation are earlier, more continuous and smoother than in Hudson Bay. In Hudson Bay, ice decay and formation are delayed, but suddenly accelerate during late spring and late autumn.

b *The SIC Signatures of the SO and the NAO*

To construct composite SIC maps of High/Dry and Low/Wet events associated with the SO, we use data from those High/Dry and Low/Wet years that have been identified by van Loon and Madden (1981) and Rogers (1984) (see the first two columns in Table 1). Since the normalized Tahiti-Darwin SLP difference (SOI) is a good measure of the SO for use in statistical diagnostic studies (Chen, 1982), we use the conventional SOI for the spectral analysis. The positive and negative values of the SOI generally correspond to the High/Dry and Low/Wet SO events, respectively, of van Loon and Madden (1981). We also list in Table 1 (the last two columns) the NAO winter events as defined by Rogers (1984). These are called weak westerlies, which occur during weak Icelandic Lows (when the NAO index is lower than −1), and strong westerlies, which occur during deepened Icelandic Lows (when the NAO index is higher than +1) (see Fig. 1 in Rogers, 1984).

Figure 4 shows the composite SIC mean of the first-year summer for 12 Low/Wet (SOI < 0) episodes listed in Table 1. (The composite SIC mean for the High/Dry events is not shown, since it is close to the summer climatology shown in Fig. 2). The second-year winter and spring composite SIC maps do not show any noticeable anomalies owing to the completely ice-covered conditions during these two seasons. Upon comparing Fig. 4 with the summer climatology in Fig. 2b, we observe that heavy sea-ice conditions occur in summer in Hudson Bay, corresponding to the

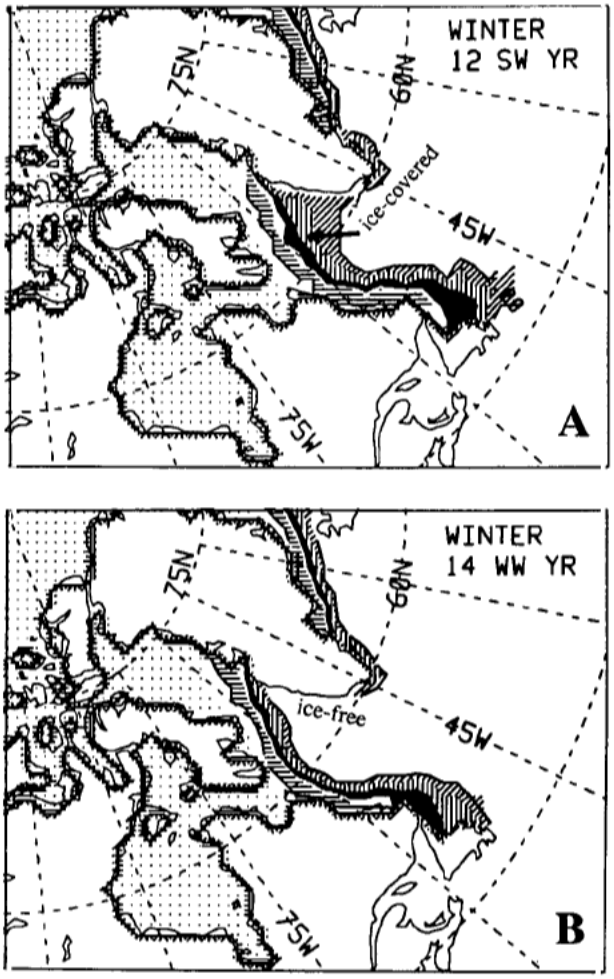

Fig. 5 The composite SIC mean in winter of (a) the 12 SW events, and (b) the 14 WW events, defined in Table 1.

Low/Wet conditions (high precipitation) in the tropical Pacific when generally SOI < 0. A comparison of the composite autumn maps (not shown) also shows that sea ice forms faster from north to south during Low/Wet events than during High/Dry events. The ice edge in Hudson Bay and Baffin Bay advances farther southward during the Low/Wet events compared with that during the High/Dry events.

Figure 5 shows the composite winter SIC during 12 strong westerly (SW) events (Fig. 5a) and 14 weak westerly (WW) events (Fig. 5b). Spring composite maps (not shown) also have the same features. The winter composite maps show that for both types of events, the ice cover in Hudson Bay is similar to climatology owing to the complete ice cover there during winter. To the west of Greenland, however,

ice-free conditions occur for the WW events (Fig. 5b) and ice-covered conditions, for the SW events (Fig. 5a). The interpretation of these results will be given below.

c *Spatial anomalies of the SIC, SLP and SAT*

To search for mechanisms explaining the above positive and negative sea-ice anomalies in the Hudson Bay and Baffin Bay–Labrador Sea region, we first examined the anomalies of the SLP, which indicate the wind anomalies of the surface atmospheric circulation, and then the SAT, which is advected by the circulation.

Figure 6 shows the composite winter SAT anomalies for the SW and WW events associated with the NAO (Table 1). It can be seen that the SAT anomalies (Figs 6a and b) are opposite in sign. Upon comparison with the composite SLP maps (not shown), we find that the negative (positive) SAT anomalies correspond to a deepened (weak) Icelandic Low. For deepened Icelandic Lows (SW events), the SAT has two large negative anomaly centres, one over Baffin Island (−3.3°C) and the other over western Greenland (−2.9°C). Negative SAT anomalies lead to a higher production of sea ice in the area. By contrast, for weak Icelandic Lows (WW events) (see Fig. 6b), the SAT has positive anomalies over the study region, with two positive centres located in approximately the same positions as the negative anomaly centres. The positive anomaly values are 2.5 and 3.6°C for Baffin Island and western Greenland, respectively. It is also interesting to note the existence of a negative anomaly of −1.0°C centred over Baffin Bay; the cause of this cool spot is unknown.

To determine the statistical significance of these results, we performed a *t*-test of the SLP and SAT fields using the methodology of van Loon and Rogers (1978). Figure 7 shows the difference between the SW and WW events (Fig. 7a) and the areas that are over the 95% significance level (Fig. 7b); these areas cover the Labrador Sea, a portion of Hudson Bay, but not Baffin Bay. We see the dipole structure between the study region and Europe. The *t*-test of the SLP field (not shown) shows a 95% significance area in the Icelandic region. These results are consistent with those found by van Loon and Rogers (1978) in terms of the well known "see-saw". A deepened Icelandic Low event of the NAO can efficiently transport northward the Atlantic moist/warm air to the European sector and advect southward the dry/cold Arctic air to the Greenland–Hudson Bay area. A weakened Icelandic Low has the opposite effect. Thus, the air temperatures to the west of Greenland alternate ("see-saw") between relatively cold and warm values.

Figure 8 shows the composite monthly means of the SOI and the composite anomalies of sea-ice area and SAT in Hudson Bay for 12 Low/Wet and 10 High/Dry events lasting over a 2-year period (Table 1). It can be seen that the SOI for the Low/Wet events generally has a sign opposite to that of the index for the High/Dry events, with extremes occurring in second-year February. From the sea-ice plots, we observe that there are positive (negative) anomalies from June to December in the first year corresponding to the Low/Wet (High/Dry) events. During January–March of the second year, these two types of events do not seem to have different SICs. At the onset of the Low/Wet phase of the SO, there is a negative SAT anomaly

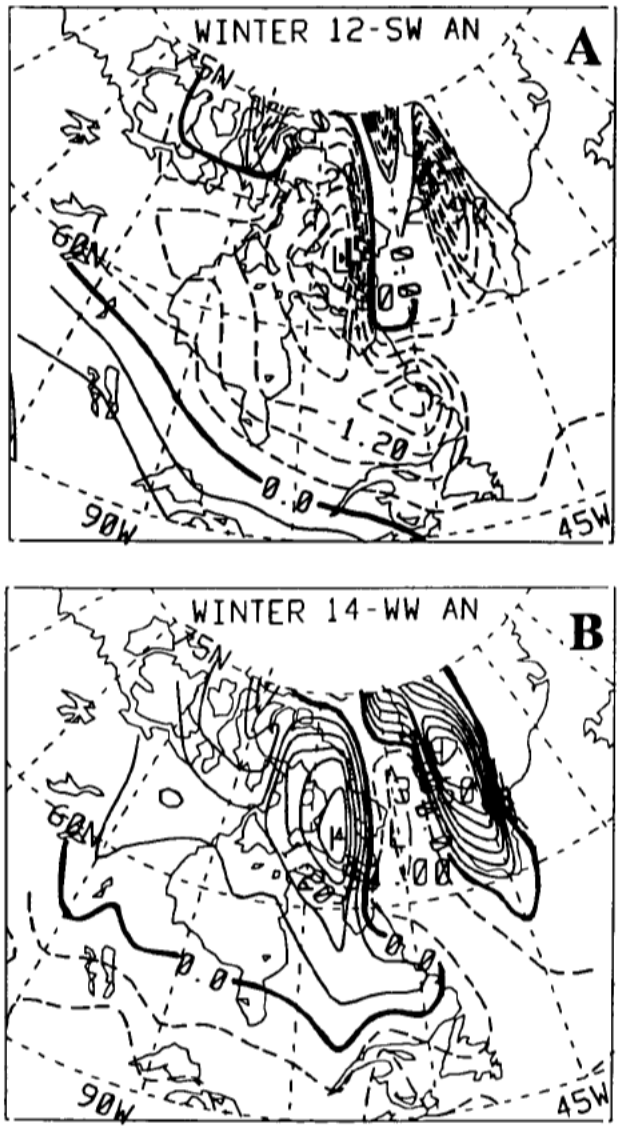

Fig. 6 The winter SAT anomalies for (a) the 12 SW events, and (b) the 14 WW events. The contour interval is 0.4°C. The solid (dashed) curves denote the positive (negative) anomalies in SAT.

for the first year, with a maximum in August. This could contribute to faster and thicker sea-ice formation before the upcoming winter. The opposite scenario can be seen for the High/Dry events. Similar features are also found for the Baffin Bay–Labrador Sea region (not shown).

To find the statistical significance, the same *t*-test of the seasonal SLP and SAT

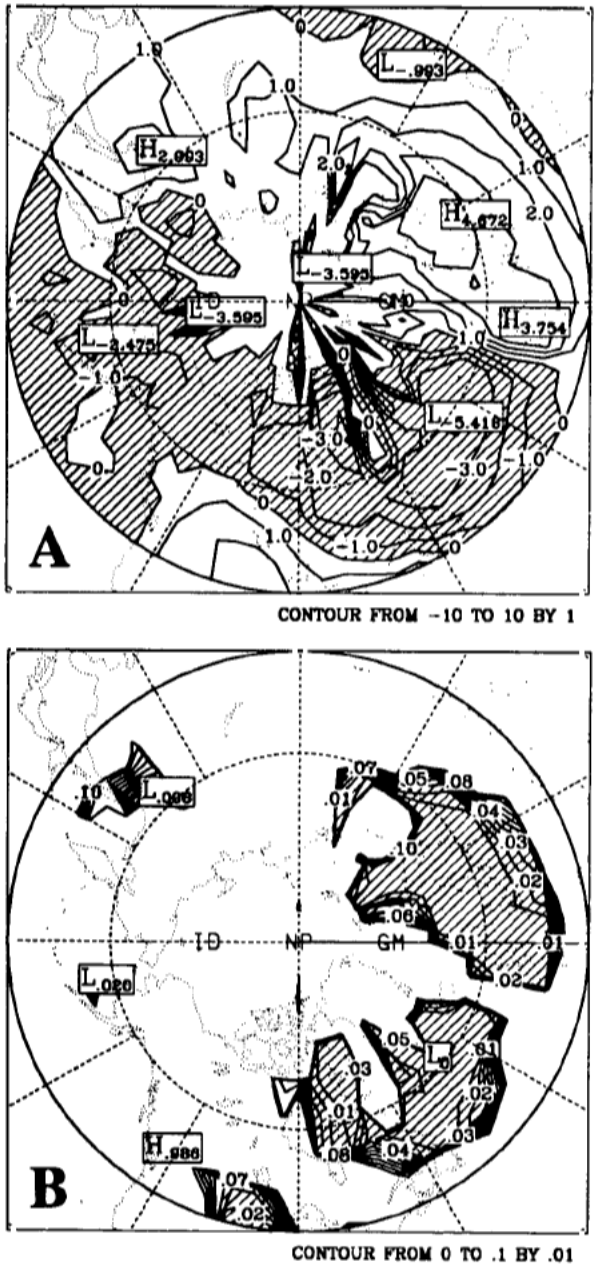

Fig. 7 (a) The winter normalized SAT difference between 12 SW and 14 WW NAO events; the contour interval is 1°C and hatched areas denote negative values. (b) The areas over 95% significance, as determined from a *t*-test are hatched; the contours range from 0.0 (100%) to 0.1 (90%) with interval 0.01.

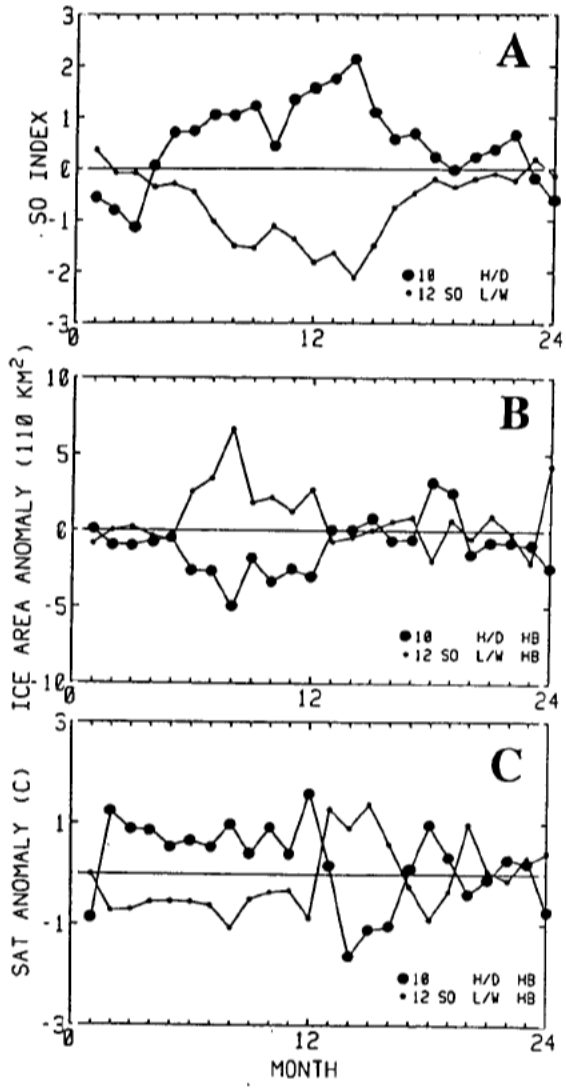

Fig. 8 The composite monthly means of the Southern Oscillation index; and the composite anomalies of (b) sea-ice area and (c) SAT in Hudson Bay for 12 Low/Wet and 10 High/Dry events. The two-year periods used to make the above composite time series are listed in Table 1. The ice area is defined as the grid-point area times the SIC in tenths.

fields as used in Fig. 7 was carried out for Low/Wet and High/Dry events from the first year to the second year of the SO. Only in the first-year summer is the statistical significance above 95%. Figure 9a shows the SAT difference of the 12 Low/Wet and 10 High/Dry events (Table 1), and Fig. 9b, the areas of 95% significance level.

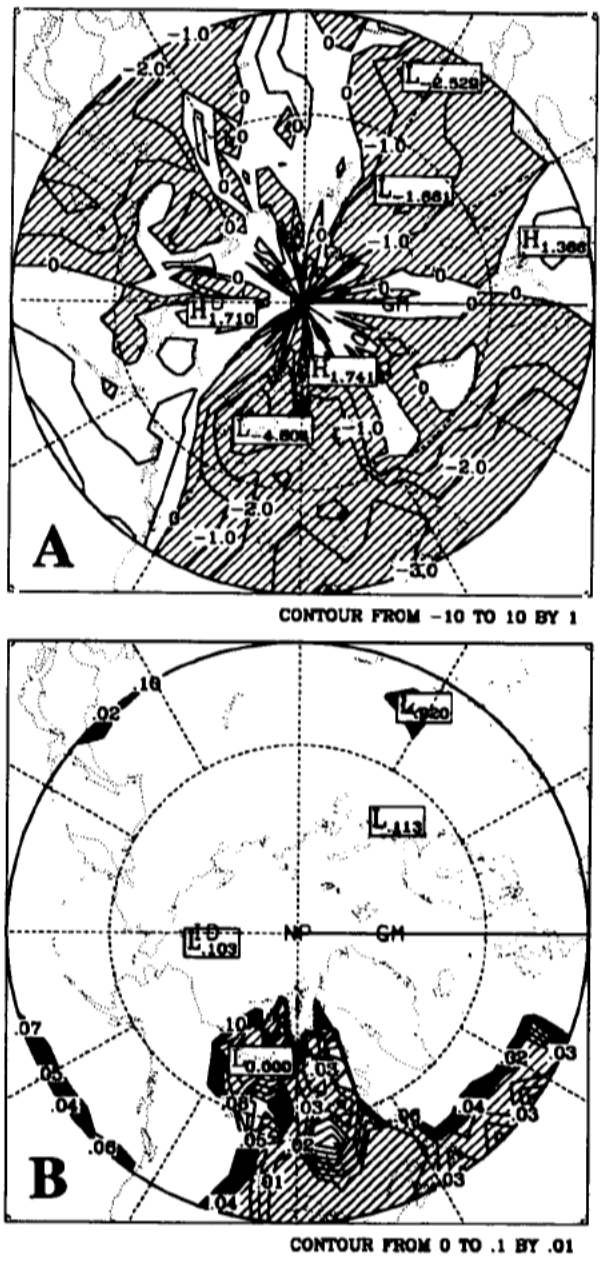

Fig. 9 Same as Fig. 7, except for the first-year summer normalized SAT difference between 12 Low/Wet and 10 High/Dry SO events.

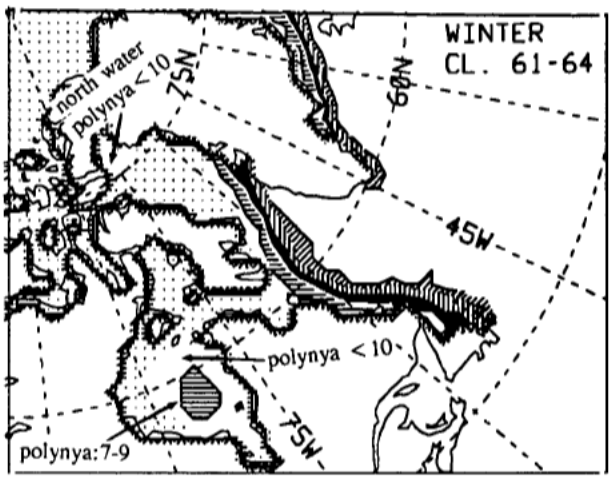

Fig. 10 The composite winter SIC mean for the short-term period 1961–64, which spans the "climate jump".

These results are consistent with Fig. 4. In the first-year autumn, there is also a negative SAT difference pattern in the study region; however, it is not above the 95% significance level.

d *The SIC Signature of a Short-Term "Climatic Jump"*

To examine short-term climatic changes of sea ice in the study region, three 4-year SIC means (1957–60, 1961–64 and 1965–68) were constructed in view of the early 1960s "climatic jump" that was marked by the sudden appearance of negative anomalies in Northern Hemisphere 500-mb heights (Knox et al., 1988; Shabbar et al., 1990). The atlas by Wang and Mysak (1991) showed that there were also substantial changes in SIC in Hudson Bay and northern Baffin Bay in the early 1960s.

Figure 10 shows the 4-year winter mean for 1961–64. The maps for the preceding and subsequent 4-year periods, 1957–60 and 1965–68, respectively, are not shown because they are close to climatology (Fig. 2). The main difference between the middle period and the other two periods is that there were polynyas in the central Hudson Bay region during 1961–64 in both winter (Fig. 10) and spring (not shown). There were also ice-free conditions in winter and spring to the west of Greenland in the middle period, but heavy ice conditions there in the other two periods. More significantly, during the middle period there was also a "North Water" polynya (with SIC less than 10/10) in northern Baffin Bay in winter, but not in the winters of the other periods (cf. Fig. 2). We also carried out the *t*-test of both SLP and SAT fields, but did not obtain a 95% statistical significance for this event. The winter SAT (not shown) was lower during 1961–64 than during the other periods. Runoff data records are not long enough to connect the sea-ice deficit during this period

to the "climate jump". However, we will show in Section 6 that sea ice in Hudson Bay is correlated with runoff, with a 1-year lag.

5 Temporal variations of the SIC, SLP and SAT

The above results show that heavy sea-ice conditions in the study region during summer are generally in phase with the onset of Low/Wet episodes of the SO. We now examine the temporal variations in SIC associated with the SO and NAO, both in the time and frequency domains. Because Hudson Bay is an almost closed region, whereas the Baffin Bay-Labrador Sea has an open boundary and hence no boundary constraint on the growth of sea ice, we consider these two regions separately.

a *Time Series of the Sea-Ice Areas*

The winter and spring sea-ice area time series for Hudson Bay (Fig. 11) are much less variable than those in summer and autumn because of the boundary constraint described above. Thus, heavy winter/spring ice conditions in Hudson Bay cannot generally be detected using SIC. However, the winter polynyas seen in Fig. 10 do show up clearly as a dip in the time series during the period 1961–64. Winter and spring ice-area time series for the Beaufort, Chukchi, East Siberian and Laptev seas (Walsh and Johnson, 1979a; Mysak and Manak, 1989) also show little variability because of the boundary constraint. Thus, ice thickness data have to be used to detect sea-ice changes during anomalous atmospheric conditions in winter and spring, as will be seen in Section 6. By contrast, large-amplitude fluctuations associated with the Low/Wet events can be found in the summer and autumn series.

A different pattern occurs for the Baffin Bay–Labrador Sea ice time series (Fig. 12). In the absence of a boundary constraint to the south, sea-ice extent in any season can change with atmospheric conditions. The variations in winter and spring are significantly larger than those in summer and autumn, in contrast to events in Hudson Bay. Thus, one can clearly discern the signatures of the Low/Wet episodes from the winter and spring time series of the sea-ice area. The summer and autumn ice-area variations also reflect the occurrence of strong Low/Wet events, but not as clearly as in Hudson Bay. The signature due to strong westerly NAO events in winter is also seen. For example, the large winter 1984 peak is due to the strong westerlies associated with the 1984 NAO event (see Table 1).

b *Time-scales of Sea-Ice Variations*

To further understand the impact of the SO and NAO on sea ice, we use spectral analysis to determine at which time-scales sea ice responds to the SO and NAO. The monthly anomalies in SIC, SAT and SLP throughout this study were obtained by subtracting the seasonal cycle (as described in Section 4a) from the monthly series. The spectra were computed for all frequency bands, but are only plotted at periods over one year. The first-order autoregressive (AR) process was applied to determine the confidence levels for a random process with two degrees of freedom in all

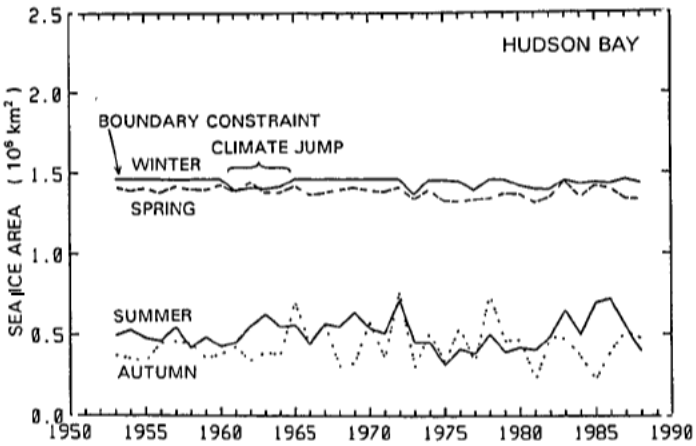

Fig. 11 The time series of sea-ice areas for the four seasons in Hudson Bay. Note that there are less variations in sea-ice area in winter and spring owing to the boundary constraint.

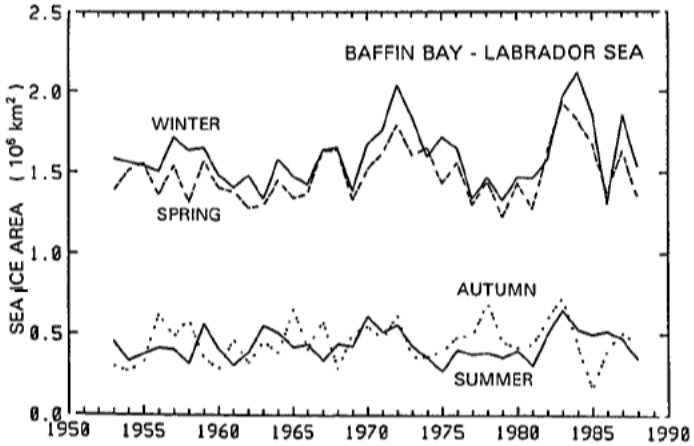

Fig. 12 Same as Figure 11, except for the Baffin Bay–Labrador Sea region.

computations (Mitchell et al., 1966; Walsh and Johnson, 1979b). The confidence limits for the co-spectra were obtained by applying the same AR process to the average of the two series. Before computation, all series were normalized by their own standard deviations.

Since the boundary constrains sea-ice growth during winter in Hudson Bay, and the NAO index is generally not defined outside winter, we only calculated the co-spectra between Baffin Bay–Labrador Sea ice-area and SO index, and also SAT. Figure 13 shows the resulting co-spectrum for the SOI. We note that sea-

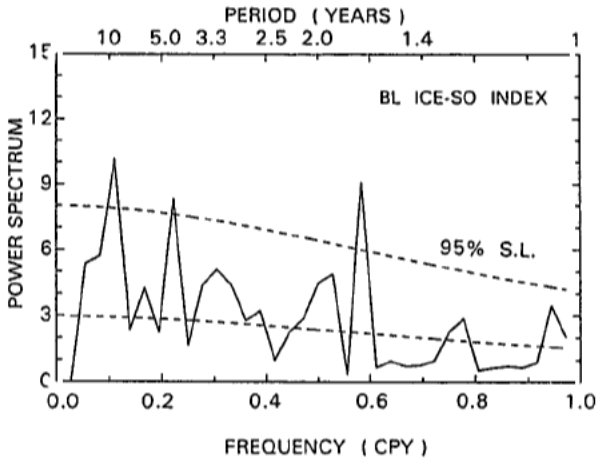

Fig. 13 The co-spectrum (solid curve) between the sea-ice area anomaly in the Baffin Bay–Labrador Sea region and the SO index. The upper (lower) dashed curve denotes the 95% confidence limit (red noise spectrum). Since the time series in this paper have been normalized by their own standard deviations, the units of the co-spectrum are in CPY^{-1} (1/cycles per year).

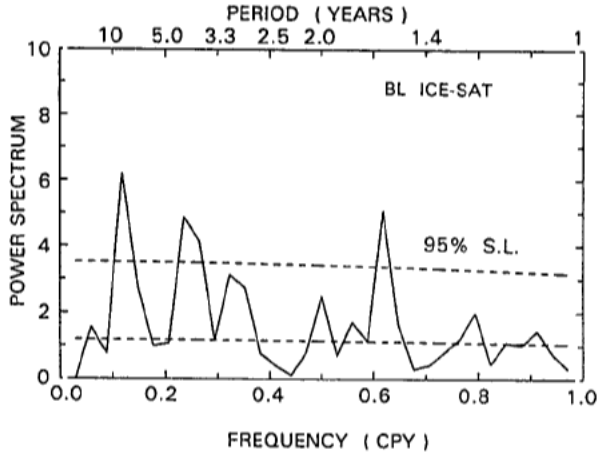

Fig. 14 Same as Fig. 13, except for the sea-ice area anomaly (solid curve) and the SAT in the Baffin Bay–Labrador Sea region.

ice fluctuations respond to the SO at about 1.7-, 5- and 10-year periods. The first two time-scales are consistent with those of ENSO as determined by Barnett (1991). The decadal time-scale is intriguing and does not appear to correspond to any known atmosphere-ocean oscillation in the tropical Pacific. Clearly it deserves further study. Figure 14 shows the co-spectra for the SAT: the response has peaks at about 1.7-, 4- and 8–10-year periods.

TABLE 2. Simultaneous and lagged correlation coefficients between sea-ice area in Hudson Bay (HB) and the Baffin Bay-Labrador Sea (BL) region, and the SO index on the NAO index and their 95% significance level (S.L.) determined by a Monte Carlo simulation. Correlations above 95% S.L. are italicized

Statistic	Winter	Spring	Summer	Autumn	Annual
Simultaneous HB Ice and SO Index					
CORR.	−0.03	−0.04	*−0.33*	−0.26	*−0.39*
95% S.L.	0.34	0.33	0.32	0.32	0.32
Summer HB Ice and SO Index					
CORR.	−0.17	−0.17	*−0.33*	*−0.33*	*−0.35*
95% S.L.	0.34	0.30	0.32	0.32	0.32
Simultaneous BL Ice and SO Index					
CORR.	−0.14	−0.03	*−0.39*	−0.28	−0.23
95% S.L.	0.34	0.31	0.30	0.28	0.33
Summer BL Ice and SO Index					
CORR.	0.33	−0.12	*−0.39*	−0.15	*−0.34*
95% S.L.	0.33	0.33	0.30	0.31	0.33
Simultaneous HB Ice and NAO Index					
CORR.	−0.34	−0.19	0.08	0.14	0.10
95% S.L.	0.38	0.29	0.35	0.32	0.30
Simultaneous BL Ice and NAO Index					
CORR.	*0.49*	0.26	0.06	0.17	*0.35*
95% S.L.	0.41	0.34	0.36	0.33	0.32

6 Correlation analysis and verification from other data sources

a *Temporal Correlation Analysis Using a Monte Carlo Simulation*

To obtain a quantitative measure of the relationships among three types of variables (sea ice, SLP gradients and SAT), cross-correlations of the seasonal and annual time series were carried out (Table 2). The significance level in this study is estimated by a Monte Carlo simulation (Livezey and Chen, 1983; Peng and Mysak, 1993). This method includes four basic steps: (a) randomize one of the original time series; (b) retrieve the original lag −1 autocorrelation in all random series; (c) calculate the correlation coefficients between the original time series and the random series; and (d) find the critical value at which only 5% of the coefficients obtained in (c) are above this value, the significance level. Only correlations above the statistical significance of 95% are discussed below.

Table 2 (first pair of lines) shows that the simultaneous sea-ice fluctuations in Hudson Bay are negatively correlated with the SO index only for summer and annual cases. Since the summer SO index is also significantly correlated with the summer SAT (0.40), it follows for example, that a larger ice extent in Hudson Bay is likely to be mainly due to the colder air temperatures, as implied by Fig. 8. The sea-ice cover in Baffin Bay–Labrador Sea is also negatively correlated with the SO index in summer (see third pair of lines). Next we note that Hudson Bay sea ice is not correlated with the NAO index in any season (see fifth pair of lines). Finally, we note that the sea ice in the Baffin Bay–Labrador Sea region is strongly correlated

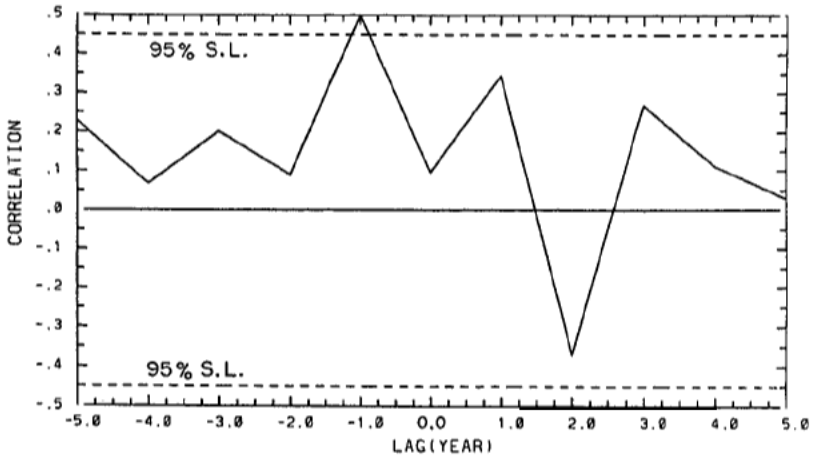

Fig. 15 The cross-correlation between the sea-ice area and the runoff in Hudson Bay. The dashed curves denote the 95% significance level obtained using a Monte Carlo simulation. A positive lag means that sea ice leads runoff.

with the NAO index in winter (0.49) (see last pair of lines), the connection likely being due to the air temperature fluctuations that are negatively correlated with the NAO winter index (−0.52).

In summary, we note that the sea-ice cover in both study regions (Hudson Bay and Baffin Bay–Labrador Sea) is correlated with the SO index in summer, whereas, only that in the Baffin Bay–Labrador Sea is correlated with the NAO index in winter. The correlation coefficients show that the NAO has a stronger link with the Baffin Bay–Labrador Sea ice (0.49, winter) than the SO index has with the Hudson Bay sea ice (−0.39, summer), indicating the NAO has a larger effect on sea ice than the SO.

Figure 15 shows the cross-correlation between Hudson Bay ice area and runoff for the period 1963–83 (the latter data were obtained from Prinsenberg et al., 1987). The only significant peak is at lag −1, indicating that sea ice in Hudson Bay is strongly correlated with runoff of the preceding year. Such a lag was also found by Manak and Mysak (1989) for sea-ice anomalies in James Bay. A similar lagged relationship with respect to Mackenzie River runoff also holds true for the sea-ice cover in the Beaufort Sea (Manak and Mysak, 1989).

b *Verification From Other Data Sources*

Annual ice thickness data (Loucks and Smith, 1989) and ice-melt dates in the spring-summer period (Etkin, 1991) are now used as independent datasets to verify the above findings for Hudson Bay. The annual time series of ice-melt fresh water in Hudson Bay during 1963–83 (not shown) also shows a pattern that is similar to the ice thickness time series (Loucks and Smith, 1989).

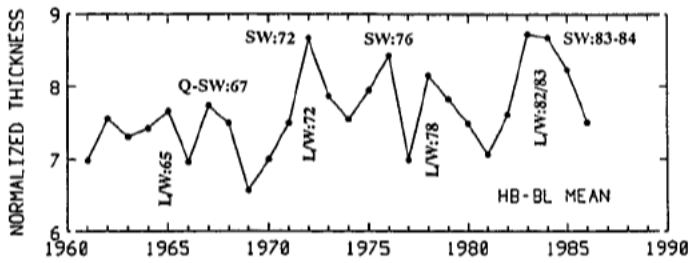

Fig. 16 The mean sea-ice thickness derived from the six ice stations shown in Fig. 1 (data from Loucks and Smith, 1989). Each time series was normalized by its own standard deviation. The peaks corresponding to the Low/Wet SO and strong westerly NAO events are marked by L/W and SW, respectively.

Figure 16 shows a time series of normalized ice thickness that was obtained by averaging data from six stations mainly around Hudson Bay (see Fig. 1) that have records from 1961 to 1986. There are noticeable peaks in 1965, 1972, 1978 and 1982/83 (4 out of 10 Low/Wet events during this period) and peaks in 1967, 1972, 1976 and 1983/84 (4 out of 10 strong westerly NAO events during this period). Note that although the year 1967 is not defined as a strong westerly NAO event by Rogers (1984) and hence is not in Table 1, we observe from his Figure 1 that the NAO index almost reaches +1, and therefore we call this a "quasi-strong" westerly event. Thus, the composite sea-ice thickness time series in the study region picks up several major signatures of both strong Low/Wet and strong westerly NAO episodes.

Figure 17 shows the 1962–86 time series of ice-melt dates at which the SIC melts to values of 5/10 in central Hudson Bay (called ice-melt dates hereafter in this section) (Etkin, 1991). It is clear that the ice-melt dates in summer are delayed in the following Low/Wet events: 1963, 1969, 1972, 1978, 1983 and 1986 (6 out of 10 Low/Wet events), and in the following strong westerly NAO events: 1967, 1972, 1976 and 1983. The same pattern was not found for the 1965/66, 1968/69 and 1977/78 Low/Wet events. The occurrence of 6 heavy ice summers in 10 Low/Wet events during this period gives support to the Low/Wet signatures found in the composite maps, as discussed in Section 4. The discrepancy in the other cases implies that other factors are significantly influencing ice conditions in Hudson Bay. One important factor may be found in Table 1: 1965/66, 1968/69 and 1977/78 Low/Wet events occur at the same time as weak westerly NAO events during the winter. From Fig. 6b, we note that there is a positive anomaly in SAT in the study region, implying that there could be lighter ice conditions during these 3 winters. Thus, the ice-melt dates advanced during these 3 events. In other words, the ice conditions in the Hudson Bay and Baffin Bay–Labrador Sea region are related to both the SO and NAO.

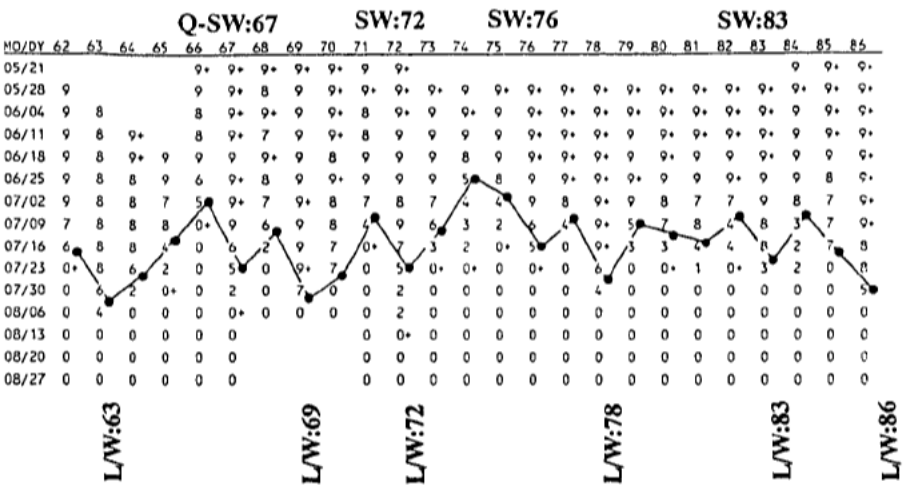

Fig. 17 The weekly ice concentration by year for central Hudson Bay. The solid line connecting the dots indicates 5/10 ice concentration (after Etkin, 1991), which represents the dates of sea-ice melting to a SIC value of 5/10. The delays (i.e. minima in the solid line curve) in melting date during the strong Low/Wet SO and strong westerly NAO events are marked by L/W and SW, respectively.

7 Case study: Large ice anomalies for 1972/73 and 1982/83 episodes

We now briefly illustrate the sea-ice response signature in the study region with respect to the strong events of 1972/73 and 1982/83, when both Low/Wet SO and strong westerly NAO events occurred, starting approximately in April of the first year of the two-year periods identified. The difference between these two events is that the 1972/73 SO index (not shown) reached its extreme negative value in May of the first year and remained negative until January of the second year, before returning to zero. The 1982/83 SOI became negative during first-year April and remained so until second-year April (Mysak, 1986), with the extreme negative value occurring in February. Note that during the 1972/73 and 1982/83 Low/Wet events, there were strong westerly NAO events in winter (Table 1).

Figure 18a shows the sea-ice and SAT anomalies in Hudson Bay for the 1972/73 and 1982/83 events. Note that a positive sea-ice anomaly extends from May to December of the first year of the 1972/73 event and then essentially disappears in the second year. By way of contrast, for the 1982/83 event, a positive sea-ice anomaly starts in first-year December and peaks in July of the second year. Note that the amplitude of the anomaly for the 1972/73 case is larger than that for the 1982/83 event. This is due in part to the colder SAT during 1972/73.

Extensive positive sea-ice anomalies in the Baffin Bay–Labrador Sea region can be clearly seen in Fig. 18b for both periods. They are quite large because of the absence of any boundary constraint. Note that the SAT anomalies in Baffin Bay

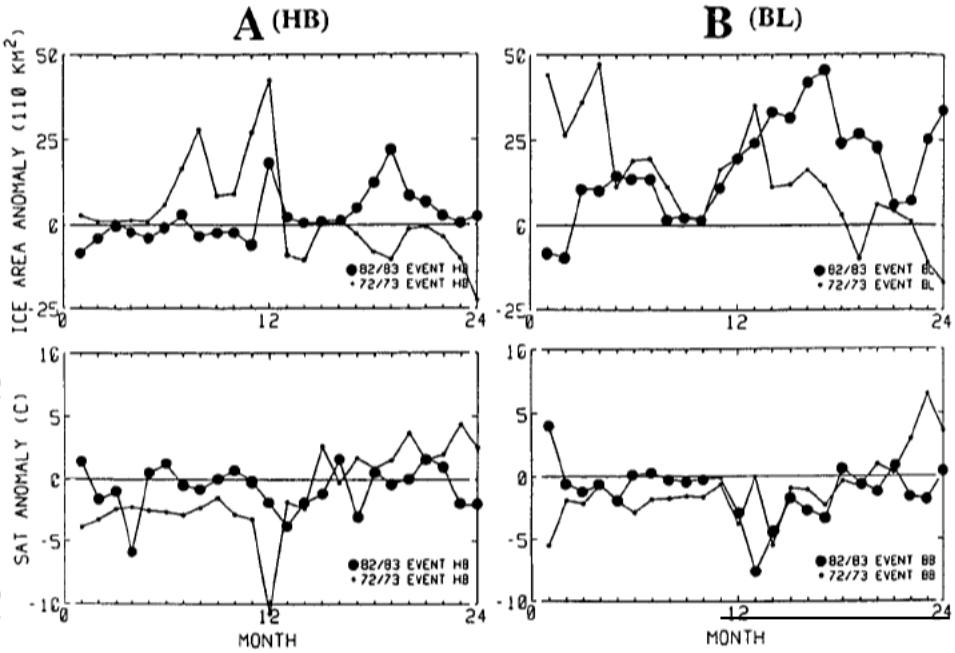

Fig. 18 The two-year (from January 1972 (1982) to December 1973 (1983)) monthly ice-area and SAT anomalies in (a) Hudson Bay, and (b) in the Baffin Bay–Labrador Sea region, for the strong Low/Wet SO events and strong westerly NAO events during 1972/73 and 1982/83.

were negative throughout most of the two-year period for both events. During these two strong Low/Wet and strong westerly events, there were also strong westerlies over the North Atlantic because of deep Icelandic Lows in the winters. This is the reason for the negative anomalies of SAT in the study regions.

It is noted that even though the 1977/78 Low/Wet SO event was larger than the 1972/73 event, according to the SO index, the ice-area and thickness anomalies in the latter event were larger than in the former. This is because during the 1977/78 Low/Wet SO event, a weak westerly NAO event occurred and this tended to oppose sea-ice enhancement in the study region.

8 Conclusions and summary

Based on the above analyses, the following conclusions can be drawn:

1) Interannual variability of sea ice in Hudson Bay, Baffin Bay and the Labrador Sea is related to large-scale atmospheric circulation (SLP) changes: the North Atlantic Oscillation and the Southern Oscillation. Sea ice has a positive anomaly during the strong westerly NAO events. However, the NAO only has an impact on sea ice in winter, and affects sea ice in the study region through "see-saw" variations in temperature (van Loon and Rogers, 1978). During the Low/Wet SO episodes, sea ice in the study region has positive anomalies in the summer of the

first year during the set-up of the episode owing to the negative anomalies in the regional surface air temperature.

2) There were noticeable changes in Hudson Bay ice cover around 1960/61 and 1964/65. The period between these years (1961–64) spanned the so-called "climate jump" of the early 1960s (Knox et al, 1988). During this period, extensive polynyas occurred in Hudson Bay, and also the North Water polynya occurred in northern Baffin Bay. However, the link between the sea-ice deficit and the "climate jump" is not clear.

3) The sea-ice cover anomalies in the Baffin Bay–Labrador Sea region respond to the SO and SAT on the following approximate time scales: 1.7-, 5- and 10-year periods.

4) Large positive anomalies in sea ice during the two strong westerly NAO and Low/Wet SO episodes of 1972/73 and 1982/83 were also found. The sea-ice anomalies in the 1972/73 (1982/83) event peaked in the first (second) year of these episodes.

5) The boundary constraint to the sea-ice growth limits what we could learn from using SIC to detect sea-ice response to changing atmospheric conditions during winter and spring in Hudson Bay. The same is probably also true for the Beaufort and Chukchi seas, and the East Siberian and Laptev seas. During strong Low/Wet and strong westerly NAO events, sea ice becomes thicker in the study region. The dates for sea-ice melt in central Hudson Bay were delayed due to positive anomalies in sea-ice volume.

6) A significant correlation between sea ice and runoff in Hudson Bay was found, with sea ice lagging by one year. However, the runoff time series is not long enough to fully determine its role in ice formation in Hudson Bay.

Acknowledgements

We express our appreciation to Dr J. Walsh for generously supplying the climate dataset from the University of Illinois and for helpful discussions during his visit to McGill. We are indebted to S. Prinsenberg, R. Loucks, R. Smith and D. Etkin for permission to use their data in our discussions. Thanks also go to Dr S. Sheng, Dr S. Peng, T. van der Baaren and A. Schwartz for their advice on data processing and technical assistance, and to Mrs U. Seidenfuss for preparing some of the figures. The discussions with Drs J. Derome, K. Higuchi and C. Lin during the course of this study are also appreciated. Finally, we thank the anonymous referees for their constructive comments and criticisms on the original draft of this paper. This study was supported by grants from NSERC and Fonds FCAR awarded to LAM and RGI, and by grants from AES and ONR awarded to LAM.

Appendix: Acronyms

ENSO El Niño/Southern Oscillation
NAO North Atlantic Oscillation

SAT	Surface Air Temperature
SIC	Sea-Ice Concentration
SLP	Sea-Level Pressure
SO	Southern Oscillation
SOI	Southern Oscillation Index
SW	Strong Westerly event of the NAO
WW	Weak Westerly event of the NAO

References

AGNEW, T. 1993. Simultaneous winter sea-ice and atmospheric circulation anomaly patterns. ATMOSPHERE-OCEAN, **31**: 259–280.

BARNETT, T.P. 1985. Variations in near-global sea level pressure. *J. Atmos. Sci.* **42**: 478–501.

———. 1991. The interaction of multiple time scales in the tropical climate system. *J. Clim.* **4**: 269–285.

BJERKNES, J. 1969. Atmospheric teleconnections from the equatorial Pacific. *Mon. Weather Rev.* **77**: 163–172.

CHEN, W.Y. 1982. Assessment of South Oscillation sea-level pressure indices. *Mon. Weather Rev.* **110**: 800–807.

DANIELSON, E.W., JR. 1969. The surface heat budget of Hudson Bay. Mar. Sci. Manusc. Rep. No. 9, McGill University, Montréal, 196 pp.

———. 1971. Hudson Bay ice conditions. *Arctic*, **24**: 90–107.

ETKIN, D.A. 1991. Break-up in Hudson Bay: Its sensitivity to air temperatures and implications for climate warming. *Climatol. Bull.* **25**: 21–34.

HIBLER III, W.D. and K. BRYAN. 1987. A diagnostic ice-ocean model. *J. Phys. Oceanogr.* **17**: 987–1015.

HOREL, J.D. and J.M. WALLACE. 1981. Planetary-scale phenomena associated with the Southern Oscillation. *Mon. Weather Rev.* **109**: 813–829.

JONES, P.D. 1988. Hemispheric surface air temperature variations: Recent trends and an update to 1987. *J. Clim.* **1**: 654–660.

KNOX, J.L.; K. HIGUCHI, A. SHABBAR and N.E. SARGENT. 1988. Secular variation of Northern Hemisphere 50 kPa geopotential height. *J. Clim.* **1**: 500–511.

LAROUCHE, P. and P.S. GALBRAITH. 1989. Factors affecting fast-ice consolidation in southeastern Hudson Bay, Canada. ATMOSPHERE-OCEAN, **27**: 367–375.

LIVEZEY, R.E. and W.Y. CHEN. 1983. Statistical field significance and its determination by Monte Carlo techniques. *Mon. Weather Rev.* **111**: 46–59.

LOUCKS, R.H. and R.E. SMITH. 1989. Hudson Bay and Ungava Bay ice-melt cycles for the period 1963–1983. Can. Contractor Rep. of Hydrogra. and Ocean Sci. No. 34, Bedford Inst. Oceanogr., 48 pp.

MANAK, D.K. and L.A. MYSAK. 1989. On the relationship between Arctic sea-ice anomalies and fluctuations in northern Canadian air temperature and river discharge. ATMOSPHERE-OCEAN, **27**: 682–691.

MARKHAM, W.E. 1986. The ice cover. In: *Canadian Inland Seas*, I.P. Martini (Ed.), Elsevier, New York, pp. 100–116.

MITCHELL, J.M.; B. DZERDZEEVSKII, H. FLOHN, W.L. HOFMEYR, H.H. LAMB, K.N. RAO and C.C. WALLEN. 1966. Climatic change. WMO Tech. Note 79, WMO-No. 195, TP 100, 79 pp.

MYSAK, L.A. 1986. El Niño, interannual variability and fisheries in the northeast Pacific Ocean. *Can. J. Fish. Aquat. Sci.* **43**: 464–497.

——— and D.K. MANAK. 1989. Arctic sea-ice extent and anomalies, 1953–1984. ATMOSPHERE-OCEAN, **27**: 376–405.

——— and S.B. POWER. 1992. Sea-ice anomalies in the western Arctic and Greenland-Iceland Sea and their relation to an interdecadal climate cycle. *Climatol. Bull.* **26**: 147–176.

———; D.K. MANAK and R.F. MARSDEN. 1990. Sea-ice anomalies observed in the Greenland and Labrador seas during 1901–1984 and their relation to an interdecadal Arctic climate cycle. *Clim. Dyn.* **5**: 111–133.

PARKINSON, C.L. 1991. Interannual variability of the spatial distribution of sea ice in the north polar region. *J. Geophys. Res.* **96**: 4791–4801.

——— and D.J. CAVALIERI. 1989. Arctic sea ice

1973–1987: Seasonal, regional, and interannual variability. *J. Geophys. Res.* **94**: 14,499–14,523.

PENG, S. and L.A. MYSAK. 1993. A teleconnection study of interannual sea surface temperature fluctuations in the northern North Atlantic and precipitation and runoff over western Siberia. *J. Clim.* **5**: 876–885.

PRINSENBERG, S.J. 1988. Ice-cover and ice-ridge contributions to the freshwater contents of Hudson Bay and Foxe Basin. *Arctic*, **41**: 6–11.

———; R.H. LOUCKS, R.E. SMITH and R.W. TRITES. 1987. Hudson Bay and Ungava Bay runoff cycles for periods 1963 to 1983. Can. Contractor Rep. of Hydrogr. and Ocean Sci. No. 92, Bedford Inst. Oceanogr., 71 pp.

ROGERS, J. 1984. The association between the North Atlantic Oscillation and the Southern Oscillation in the Northern Hemisphere. *Mon. Weather Rev.* **112**: 1999–2015.

ROGERS, J.C. and H. VAN LOON. 1979. The seesaw in winter temperatures between Greenland and northern Europe. Part II: Some oceanic and atmospheric effects in middle and high latitudes. *Mon. Weather Rev.* **107**: 509–519.

SHABBAR, A.; K. HIGUCHI and J.L. KNOX. 1990. Regional analysis of Northern Hemisphere 50 kPa geopotential heights from 1946 to 1985. *J. Clim.* **3**: 543–557.

VAN LOON, H. and R.A. MADDEN. 1981. The South Oscillation. Part I: Global associations with pressure and temperature in northern winter. *Mon. Weather Rev.* **109**: 1150–1162.

——— and J.C. ROGERS. 1978. The seesaw in winter temperatures between Greenland and northern Europe, Part I: General description. *Mon. Weather Rev.* **106**: 296–310.

WAKATA, Y. and E.S. SARACHIK. 1991. On the role of equatorial ocean modes in the ENSO cycle. *J. Phys. Oceanogr.* **21**: 434–443.

WALSH, J.E. and C.M. JOHNSON. 1979a. An analysis of sea ice fluctuations, 1953–77. *J. Phys. Oceanogr.* **9**: 580–591.

——— and ———. 1979b. Interannual atmospheric variability and associated fluctuations in Arctic sea ice extent. *J. Geophys. Res.* **84**: 6915–6928.

——— and W.L. CHAPMAN. 1990. Short-term climate variability of the Arctic. *J. Clim.* **3**: 237–250.

WANG, J. and L.A. MYSAK. 1991. Climate atlas of seasonal sea-level pressure and sea ice concentration in the Hudson Bay–Baffin Bay Labrador Sea region: 1953–1988. Centre for Climate and Global Res. Rep. 91-5, McGill University, Montréal, 103 pp.